Threshold flux-controlled memristor model and its equivalent circuit implementation*

Wu Hua-Gan(武花干)[a], Bao Bo-Cheng(包伯成)[b]†, and Chen Mo(陈 墨)[b]

[a] School of Eelctronic and Optical Engineering, Nanjing University of Science and Technology, Nanjing 210094, China
[b] School of Information Science and Engineering, Changzhou University, Changzhou 213164, China

(Received 25 March 2014; revised manuscript received 23 April 2014; published online 10 September 2014)

Modeling a memristor is an effective way to explore the memristor properties due to the fact that the memristor devices are still not commercially available for common researchers. In this paper, a physical memristive device is assumed to exist whose ionic drift direction is perpendicular to the direction of the applied voltage, upon which, corresponding to the HP charge-controlled memristor model, a novel threshold flux-controlled memristor model with a window function is proposed. The fingerprints of the proposed model are analyzed. Especially, a practical equivalent circuit of the proposed model is realized, from which the corresponding experimental fingerprints are captured. The equivalent circuit of the threshold memristor model is appropriate for various memristors based breadboard experiments.

Keywords: memristor, window function, equivalent circuit, experiment

PACS: 84.30.Bv, 84.30.–r, 05.45.–a **DOI:** 10.1088/1674-1056/23/11/118401

1. Introduction

Memristor is a nonlinear two-terminal electronic element with an adjustable resistance or conductance.[1] Due to the special features of both nonlinearity and memory,[2] memristors attract a lot of attention for potential applications in analog[3] and digital information processing,[4] neuromorphic systems,[5,6] analog circuits,[7–11] and so on.

The memristor was first postulated by Chua in 1971 based on the theory of components symmetry,[2] which relates to two fundamental circuit variables, charge q and magnetic flux φ. According to the independent variable, a memristor is defined as charge-controlled or flux-controlled, and its constitutive relation is expressed as $\varphi = \hat{\varphi}(q)$ or $q = \hat{q}(\varphi)$, respectively. The corresponding voltage–current relation can be expressed as $v(t) = R_{\rm M}(q)i(t)$ or $i(t) = G_{\rm M}(\varphi)v(t)$, where $R_{\rm M}(q) = {\rm d}\hat{\varphi}(q)/{\rm d}q$ and $G_{\rm M}(\varphi) = {\rm d}\hat{q}(\varphi)/{\rm d}\varphi$ stand for the memristance and the memductance, respectively.[1] In electrical engineering, duals refer to pairs of electrical terms that are associated together.[12] A dual of a relationship can be easily obtained by interchanging voltage and current in an expression, such as resistance R and conductance G, capacitance C and inductance L, etc. Thus, memristance $R_{\rm M}(q)$ and memductance $G_{\rm M}(\varphi)$ are also a pair of duals. From this perspective, a charge-controlled memristor and a flux-controlled memristor can be duals if their mathematical models can be transformed into each other by interchanging voltage and current.

Although the Hewlett-Packard (HP) Lab has announced the fabrication of a memristor device,[5] memristors are still commercially unavailable nowadays; perhaps this situation will continue for a long time due to the cost and the technical difficulties in fabricating nanometer-size devices. Therefore, modeling of the basic memristor[10,13–16] and designing the emulator of mem-systems make a contribution to exploring the dynamical behaviors.[17–20] The HP TiO_2 memristor is the most extensive physical device model for various research. Reference [16] presented a threshold adaptive memristor model, which is flexible and more suitable for circuit simulations. Reference [17] proposed a memristor emulator to imitate the behaviors of the HP TiO_2 memristor by using off-the-shelf components. By using a specific window function, a SPICE model of the HP TiO_2 memristor with nonlinear dopant drift was demonstrated in Ref. [21]. However, these studies are all based on the charge-controlled memristor model.

In this paper, we concentrate on a threshold flux-controlled memristor model and its equivalent circuit realization. The paper is organized as follows. Firstly, we simply review the HP TiO_2 memristor model[5] and Biolek's window function.[21] Secondly, a flux-controlled memristor model with two types of linear model and threshold model is proposed based on the duality of the electrical circuit theory and the HP TiO_2 memristor model. Thirdly, the corresponding window function circuit and the basic memristor circuit are designed, for which the equivalent circuit experiment is performed. Finally, some concluding remarks are given.

*Project supported by the National Natural Science Foundation of China (Grant No. 51277017) and the Natural Science Foundation of Jiangsu Province, China (Grant No. BK2012583).

†Corresponding author. E-mail: mervinbao@126.com

© 2014 Chinese Physical Society and IOP Publishing Ltd

2. HP TiO_2 memristor model

As described in Ref. [5], the HP TiO_2 memristor model is a linear ion drift model. The device of physical width D contains two regions, the doped region of width w and the undoped region of width $D-w$. By applying an external bias $v(t)$ across the device, the charged dopants are forced to drift in the direction of the external voltage, the boundary between the two regions moves. Each region can be equivalent to a variable resistor, thus the total resistance of the device is the sum of two variable resistors connected in a series, as shown in Fig. 1(a).

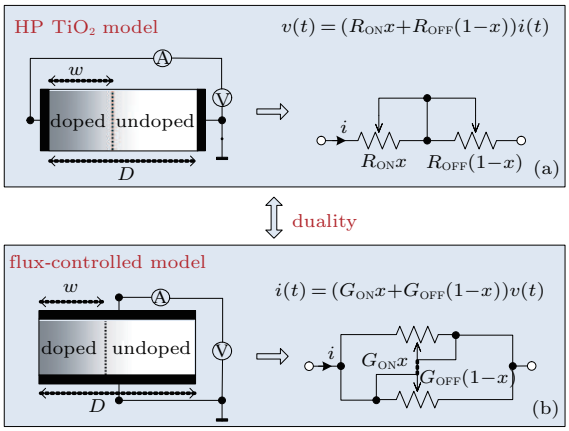


Fig. 1. (color online) The relationship of duality between two models: (a) the HP TiO_2 memristor model; (b) a flux-controlled memristor model.

This HP TiO_2 memristor model is described as

$$v(t) = R_{\mathrm{M}} i(t), \tag{1}$$

$$R_{\mathrm{M}} = R_{\mathrm{ON}} x + R_{\mathrm{OFF}} (1-x), \tag{2}$$

$$\frac{\mathrm{d}x}{\mathrm{d}t} = K_i i(t), \tag{3}$$

where R_{M} is the memristance, $x = w(t)/D \in (0,1)$, and $K_i = \mu_v R_{\mathrm{ON}}/D^2$ is the system parameter of the memristor. The definitions of other variables are consistent with those in Ref. [5].

In a nanoscale device, enormous electric fields can be yielded by a small voltage.[5] The phenomenon of nonlinear dopant drift exists especially at the boundary between the doped and the undoped regions, known as the boundary effects. Several window functions have been proposed to deal with the boundary effects.[16,21,22] The window function proposed by Biolek[21] depends not only on x but also on the sign of the current $i(t)$ through the memristor, which is in the following form:

$$F_i(x) = 1 - [x - \mathrm{stp}(-i)]^{2p}, \tag{4}$$

where p is a positive integer, and

$$\mathrm{stp}(i) = \begin{cases} 1, & i \geq 0, \\ 0, & i < 0. \end{cases} \tag{5}$$

Hence, $F_i(x)$ in Eq. (4) is regarded as a current-type window function. When the right of Eq. (3) is multiplied by the window function in Eq. (4), the memristor model of Eqs. (1)–(3) becomes a threshold one.

3. Threshold flux-controlled memristor model

3.1. Flux-controlled memristor model

Memory effects are ubiquitous in nature and particularly in nano-materials.[23] Corresponding to the HP TiO_2 memristor device, a physical memristive device of the flux-controlled memristor is assumed to exist whose ionic drift direction is perpendicular to the direction of the applied voltage, as shown in Fig. 1(b).

This device is also composed of two regions with different conductivity values: the doped region of width w and the undoped one of width $D-w$. The boundary between the two regions moves in the orthogonal direction of the external voltage on the assumption that the device can be simplified as two variable conductors G_{ON} and G_{OFF} connected in parallel, G_{ON} and G_{OFF} refer to the different conductances of the doped and the undoped regions, respectively. A conductor is a type of material to permit the flow of electric charge. When the boundary reaches the left end ($x = 0$), the conductor G_{ON} states in open circuit, thus $G_{\mathrm{M}} = G_{\mathrm{OFF}}$, and when the boundary reaches the right end ($x = 1$), the conductor G_{OFF} states in an open circuit, $G_{\mathrm{M}} = G_{\mathrm{ON}}$. Note that the simplified circuit in Fig. 1(b) becomes invalid in the case of $x = 0$ or $x = 1$. The flux-controlled memristor model can be proposed as

$$i(t) = G_{\mathrm{M}} v(t), \tag{6}$$

$$G_{\mathrm{M}} = G_{\mathrm{ON}} x + G_{\mathrm{OFF}} (1-x), \tag{7}$$

$$\frac{\mathrm{d}x}{\mathrm{d}t} = K_v F_v(x) v(t), \tag{8}$$

where $K_v = \mu_v / G_{\mathrm{ON}} D^2$ is the system parameter of the memristor, and $F_v(x)$ is the characteristic function. If $F_v(x)$ is a constant, the model of Eqs. (6)–(8) is linear; whereas if $F_v(x)$ represents a window function, the model is a threshold one. Comparing this model to the HP TiO_2 memristor model of Eqs. (1)–(3), we can see that one model can be obtained from the other just by interchanging voltage and current, thus they are duals of each other.

When the system parameters G_{ON} and G_{OFF} satisfy the condition $G_{\mathrm{ON}} \gg G_{\mathrm{OFF}}$, equation (7) can be simplified as

$$G_{\mathrm{M}} = G_{\mathrm{OFF}} + G_{\mathrm{ON}} x. \tag{9}$$

3.2. Linear flux-controlled memristor model

When $F_v(x) = 1$, the model of Eqs. (6)–(8) is a linear flux-controlled memristor model. Consider that the system parameters are $K_v = 10^3$, $G_{\mathrm{ON}} = 1$ mS, $G_{\mathrm{OFF}} = 10$ μS, and an external sinusoidal voltage stimulus

$$v(t) = V_{\mathrm{m}} \sin(2\pi f t) \tag{10}$$

is connected across the memristor. Here V_m is the amplitude and f is the frequency. When $V_m = 1$ V and f is selected as 500 Hz, 1 kHz, and 10 kHz respectively, the device can exhibit a pinched hysteresis loop, as shown in Fig. 2(a). Correspondingly, the relationship between v and the memductance G_M is depicted in Fig. 2(b).

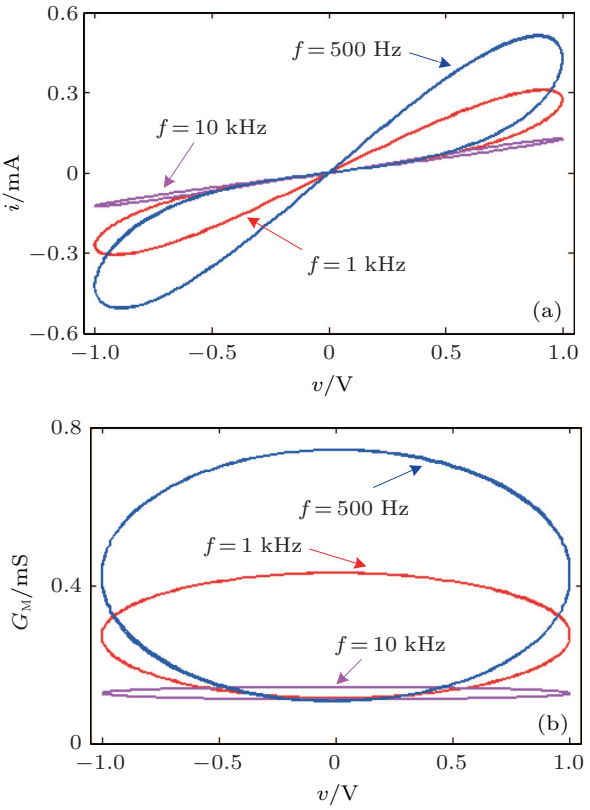


Fig. 2. (color online) Properties of the linear flux-controlled memristor model with $x(0) = 0.1$: (a) v–i curves with different f; (b) memductance $G_M(t)$ with different f.

The pinched hysteresis loop is shrunk as the stimulus frequency f increases from 500 Hz to 10 kHz. When f increases toward infinity, the pinched hysteresis loop will become a single-valued function. The dynamic range of the memductance is also shrunk with f increasing, and eventually degenerates into a constant, which is affected by the initial state of x.

3.3. Threshold flux-controlled memristor model

When $F_v(x)$ in Eq. (8) is a window function to deal with the boundary effects, the model of Eqs. (6)–(8) is a threshold flux-controlled memristor model. Similar to Eq. (4), a window function $F_v(x)$ is assumed as

$$F_v(x) = 1 - [x - \mathrm{stp}(-v)]^{2p}, \tag{11}$$

where p is a positive integer, v is the voltage across the memristor, and

$$\mathrm{stp}(v) = \begin{cases} 1, & v \geq 0, \\ 0, & v < 0. \end{cases} \tag{12}$$

Contrasting with the current-type window function, $F_v(x)$ in Eq. (11) can be regarded as a voltage-type window function. In this work, $p = 1$ is adopted; the corresponding window function is shown in Fig. 3. Because of the window function, the ionic drift mobility at the edges between the doped and the undoped regions is zero. Intuitive effects can be reflected from x, which is well restricted in the (0, 1) region.

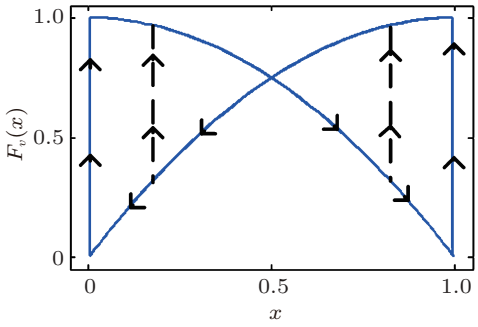


Fig. 3. (color online) Window function described by Eq. (11) with $p = 1$.

When the same system parameters are selected and a sinusoidal voltage stimulus of Eq. (10) is applied, the properties of the threshold model are shown in Fig. 4. Figure 4(a) indicates that the threshold model exhibits a hysteresis loop, which is pinched at the origin, and the hysteresis lobe area decreases with the increase of the frequency. From Fig. 4(b), it can be seen that the dynamic range of the memductance decreases with the increase of the frequency, and when the frequency tends to 10 kHz or more, the memductance regresses to a normal conductance.

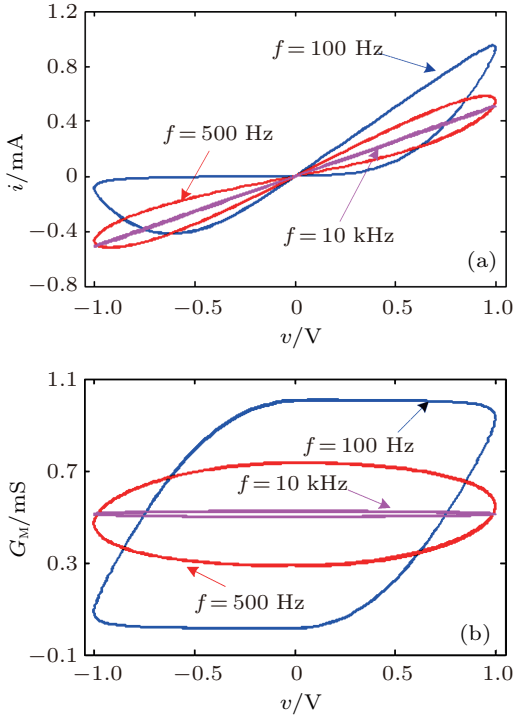


Fig. 4. (color online) Properties of threshold flux-controlled memristor model with $x(0) = 0.1$: (a) v–i curves with different f; (b) memductance $G_M(t)$ with different f.

Obviously, the features of the proposed model satisfy three fingerprints of a memristor,[24] which means that the proposed model is a memristor. Additionally, it should be mentioned that the hysteresis loop of the proposed model is asymmetric at low frequency. When the frequency is low, for example 100 Hz, it can be seen that the memductance $G_{\rm M}$ holds when $G_{\rm M}$ reaches the limits $G_{\rm ON}$ or $G_{\rm OFF}$ until it returns back to the effective area in Fig. 4(b). Thus, the corresponding hysteresis loop in the v–i plane becomes asymmetric.

4. Equivalent circuit realization

4.1. Window function circuit

Assume that the operational amplifier is an ideal component, there is no current exchange between the operational amplifier and its peripheral circuit, and the two input terminals of the operational amplifier have an identical voltage, i.e., $i_+ = i_- = 0$, $v_+ = v_-$. The circuit schematic of window function $F_v(x)$ is depicted in Fig. 5.

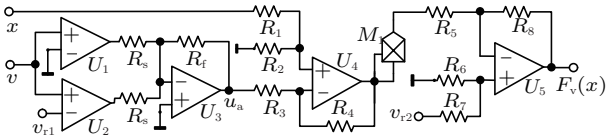


Fig. 5. Circuit schematic of the window function $F_v(x)$ in Eq. (11).

The operational amplifiers U_1 and U_2 are two comparators, and the operational amplifier U_3 connected with the resistors $R_{\rm s}$ and $R_{\rm f}$ forms an adder circuit. The resistors are configured to satisfy the conditions $R_{\rm s} = E_{\rm s}$ kΩ and $R_{\rm f} = 0.5$ kΩ, where $E_{\rm s}$ is the saturated output voltage of the operational amplifier U_1. The voltage $v_{\rm r1}$ is a DC voltage, which is larger than the maximum of $v(t)$. Thus, the output of U_2 always equals to $E_{\rm s}$ V. Here we set $v_{\rm r1}$ to be 5 V.

Thus, the output $u_{\rm a}$ of the operational amplifier U_3 is obtained by

$$u_{\rm a} = 0.5\,(\mathrm{sgn}(v) - 1) = \mathrm{stp}(-v). \tag{13}$$

The rest of the circuit in Fig. 5 is composed of two subtraction circuits and a multiplying circuit. The voltage $v_{\rm r2}$ is a DC voltage valued 1 V. By configuring $R_1 = R_2 = R_3 = R_4$ and $R_5 = R_6 = R_7 = R_8$, the output of the operational amplifier U_5 can be obtained by

$$F_v(x) = 1 - g_1(x - u_{\rm a})^2 = 1 - g_1\,[x - \mathrm{stp}(-v)]^2, \tag{14}$$

where g_1 is the scale factor of the multiplier M_1.

4.2. Basic circuit

The basic circuit of the flux-controlled memristor model is designed as shown in Fig. 6, which is composed of two multipliers (labeled M_2 and M_3), three operational amplifiers (labeled U_6, U_7, and U_8), and several discrete components. Two scale factors of the multipliers M_2 and M_3 are denoted as g_2 and g_3, respectively. All of the operational amplifiers in Figs. 5 and 6 have the same circuit characteristics.

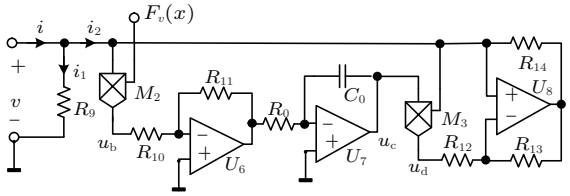


Fig. 6. Circuit schematic of the novel flux-controlled memristor.

The operational amplifier U_6 with resistors R_{10} and R_{11} is used as a reverse proportional amplifier, and U_7 connecting with resistor R_0 and capacitor C_0 is an integrator. The operational amplifier U_8 connecting with R_{12}, R_{13}, and R_{14} is a current inverter. Thus, the memristance of the equivalent circuit can be easily calculated by

$$G_{\rm M} = \frac{1}{R_9} - \frac{1}{R_{12}} + \frac{g_3}{R_{12}} u_{\rm c}. \tag{15}$$

Here, we select voltage $u_{\rm c}$ to stand for x. By comparing Eq. (15) with Eq. (9), we can obtain

$$\frac{1}{R_9} - \frac{1}{R_{12}} = G_{\rm OFF}, \quad \frac{g_3}{R_{12}} = G_{\rm ON}. \tag{16}$$

In the circuit implementation of the memristor model of Eqs. (6)–(8), $F_v(x) = 1$ can be easily achieved by applying a DC voltage valued 1 V, and $F_v(x)$ described in Eq. (11) can be achieved by using the circuit module shown in Fig. 5.

4.3. Experimental results

Analog multiplier AD633JN and operational amplifier AD711KN are used in the circuit experiment, with operation voltages of ±15 V. In this condition, the saturated output voltage $E_{\rm sat}$ of the operational amplifier is measured to be 12.7 V. The physical circuit setup is shown in Fig. 7. In our equivalent circuit implementation, the equivalent circuit parameters are listed in Table 1.

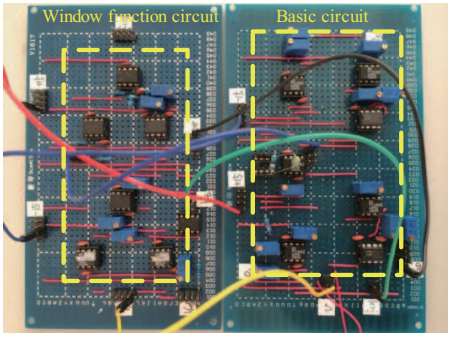


Fig. 7. (color online) Physical circuit setup.

Note that the trends of memductance G_M changing with voltage v can be depicted by the follow formula:

$$\Delta G_M = G_{ON} x = 10^{-3} x, \tag{17}$$

which is obtained from Eq. (9). The output u_c of the operational amplifier U_7 is a function of x ($x = u_c$). Thus, the corresponding numerical relationship between ΔG_M and u_c is given by

$$u_c = 10^3 \Delta G_M. \tag{18}$$

In the circuit experiment, we can measure the voltage u_c to represent the memductance ΔG_M.

Table 1. Circuit parameters of the memristor equivalent circuit.

Parameter	Signification	Value
C_0	capacitance	10 nF
R_f	resistance	0.5 kΩ
R_s	resistance	12.7 kΩ
R_0, R_1–R_8, R_{11}	resistance	10 kΩ
R_9	resistance	1 kΩ//100 kΩ
R_{10}	resistance	100 kΩ
R_{12}	resistance	1 kΩ
R_{13}, R_{14}	resistance	2 kΩ
g_1, g_2, g_3	coefficient	1

The stimulus is applied by a digital signal generator RIGOL DG2041A. A digital oscilloscope, Tektronix TDS3034c, is used to observe and capture the experimental results. Figure 8 shows an oscilloscope display of the window function measured from the equivalent circuit, which is very similar to the numerical simulation results in Fig. 3. The experimental results of the linear flux-controlled model for different frequencies at 100 Hz, 500 Hz, and 10 kHz are shown in Fig. 9, corresponding to the results in Fig. 2. The results of the threshold flux-controlled model for various frequencies at 500 Hz, 1 kHz, and 10 kHz are shown in Fig. 10, consistent with the results in Fig. 4.

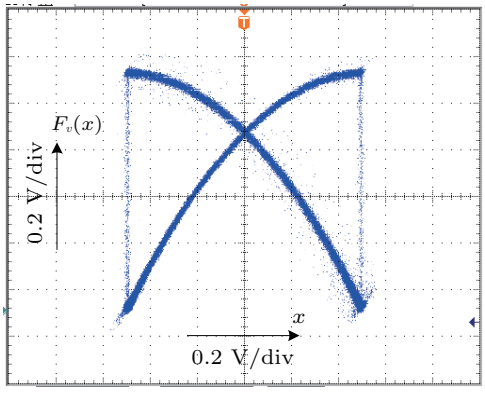


Fig. 8. (color online) Experimental results of the window function circuit.

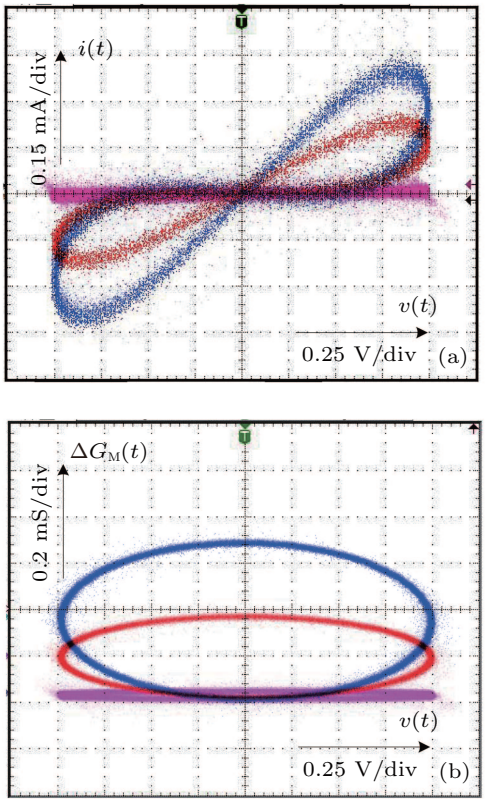


Fig. 9. (color online) Experimental results of linear flux-controlled memristor model: (a) v–i curves with different f; (b) memductance $\Delta G_M(t)$ with different f.

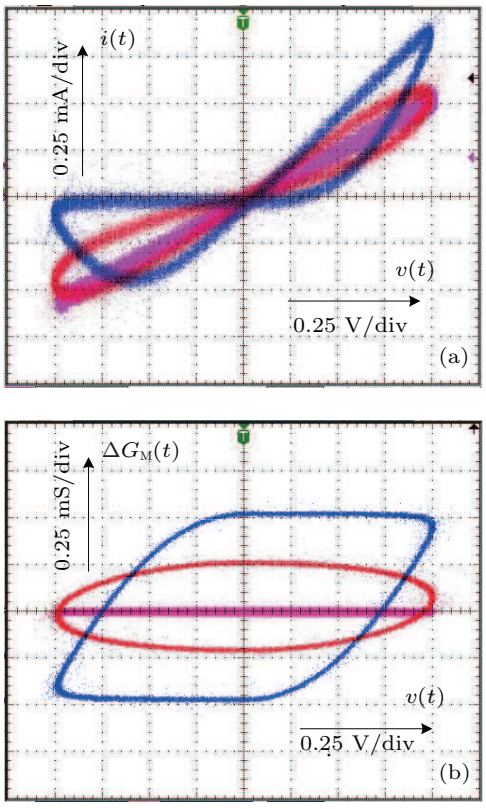


Fig. 10. (color online) Experimental results of threshold flux-controlled memristor model: (a) v–i curves with different f; (b) memductance $\Delta G_M(t)$ with different f.

5. Conclusion

In this work, a threshold flux-controlled memristor model has been proposed based on the assumption of the existence of a novel physical memristive device. The proposed model and the HP TiO_2 model are a pair of duals, they have similar properties including the pinched hysteresis loop. The corresponding equivalent circuit experimentation is performed with the basic memristor circuit and the window function circuit. From the numerical simulation results and the experimental results, we can understand the proposed memristor model better. Compared with the linear flux-controlled model, the threshold model can well restrict the memductance in a bounded region, and generate a more irregular pinched hysteresis loop at a lower frequency. Rich physical phenomena may be generated from memristor-based systems by introducing the threshold flux-controlled memristor model.

References

[1] Chua L O 2011 *Appl. Phys. A: Mater. Sci. Process* **102** 765
[2] Chua L O 1971 *IEEE Trans. Circuit Theory* **CT-18** 507
[3] Itoh M and Chua L O 2009 *Int. J. Bifurc. Chaos* **19** 3605
[4] Borghettil J, Snider G S, Kuekes P J, Yang J J, Stewart D R and Williams R S 2010 *Nature Lett.* **464** 873
[5] Strukov D B, Snider G S, Stewart D R and Williams R S 2008 *Nature* **453** 80
[6] Kim H, Sah M P, Yang C, Roska T and Chua L O 2012 *IEEE Trans. Circuit Syst. I: Regular Papers* **59** 148
[7] Wang F 2013 *IEEE Trans. Circuits Syst. I: Regular Papers* **60** 616
[8] Muthuswamy B 2010 *Int. J. Bifurc. Chaos* **20** 1335
[9] Bao B C, Xu J P, Zhou G H, Ma Z H and Zou L 2011 *Chin. Phys. B* **20** 120502
[10] Li Z J and Zheng Y C 2013 *Chin. Phys. B* **22** 040502
[11] Huang D, Wu J J and Tang Y H 2014 *Chin. Phys. B* **23** 038404
[12] Belevitch V 1962 *Proc. IRE* **50** 848
[13] Wang X Y, Fitch A L, Iu H H C, Sreeramb V and Qi W G 2012 *Chin. Phys. B* **21** 108501
[14] Fang X D, Tang Y H, Wu J J, Zhu X, Zhou J and Huang D 2013 *Chin. Phys. B* **22** 078901
[15] Li Z J, Zeng Y C and Tan Z P 2014 *Acta Phys. Sin.* **63** 098501 (in Chinese)
[16] Kvatinsky S, Friedman E G, Kolodny A and Weiser U C 2013 *IEEE Trans. Circuits Syst. I : Regular Papers* **60** 211
[17] Kim H, Sah M P, Yang C, Cho S and Chua L O 2012 *IEEE Trans. Circuits Syst. I: Regular Papers* **59** 2422
[18] Yu D S, Liang Y, Chen H and Iu H H C 2013 *IEEE Trans. Circuits Syst. II: Exp. Briefs* **60** 207
[19] Liang Y, Yu D S and Chen H 2013 *Acta Phys. Sin.* **62** 158501 (in Chinese)
[20] Wang X Y, Fitch A L, Iu H H C and Qi W G 2012 *Phys. Lett. A* **376** 394
[21] Biolek Z, Biolek D and Biolková V 2009 *Radioengineering* **18** 210
[22] Joglekar Y N and Wolf S J 2009 *Eur. J. Phys.* **30** 661
[23] Pershin Y V and Di Ventra M 2011 *Adv. Phys.* **60** 145
[24] Adhikari S P, Sah M Pd, Kim H and Chua L O 2013 *IEEE Trans. Circuits Syst. I: Regular Papers* **60** 3008